

# Performance development of styrene-butadiene copolymer-modified calcium sulfoaluminate cement mortar under different curing conditions\*

Ru WANG<sup>†1,2</sup>, Yu-sheng FAN<sup>1,2</sup>, Zhao-jia WANG<sup>3</sup>, Tian-yong HUANG<sup>3</sup>, Tao ZHANG<sup>1,2</sup>

<sup>1</sup>Key Laboratory of Advanced Civil Engineering Materials (Tongji University), Ministry of Education, Shanghai 201804, China

<sup>2</sup>School of Materials Science and Engineering, Tongji University, Shanghai 201804, China

<sup>3</sup>State Key Laboratory of Solid Waste Reuse for Building Materials, Beijing Building Materials Academy of Science Research, Beijing 100041, China

<sup>†</sup>E-mail: ruwang@tongji.edu.cn

Received Nov. 24, 2020; Revision accepted Mar. 26, 2021; Crosschecked Nov. 18, 2021

**Abstract:** The purpose of this study was to investigate the change in the physical and mechanical properties of styrene-butadiene copolymer (SB) dispersion-modified calcium sulfoaluminate (CSA) cement mortar as it aged from 28 to 360 d, and cured at different temperatures and relative humidities. The results show that the mechanical properties of reference mortar (RM) of CSA cement, including its flexural, compressive, and tensile bond strength, showed a reduction after a certain time, but its water capillary absorption was hardly affected by age. When SB dispersion was added, there was no reduction in mechanical strength. The amount of SB added did matter. Addition of 5% SB had a negative effect on most properties compared with RM, except for tensile bond strength. However, the properties of SB-modified mortar (SBMM) were enhanced significantly as the amount of SB was increased from 5% to 20%. Temperature change had different effects on the properties of RM and SBMM. High temperature was beneficial to early flexural and compressive strength development of RM, but caused serious strength reduction at later stages. High temperature enhanced the development of tensile bond strength of RM. Increasing temperature enhanced properties of SBMM, including flexural, compressive, and tensile bond strength. Higher relative humidity improved all measured properties of all mortars. Scanning electron microscope (SEM) observations of the morphology of RM and SBMM at 360 d cured under different conditions accounted well for the changes in mechanical properties.

**Key words:** Calcium sulfoaluminate (CSA) cement; Styrene-butadiene copolymer (SB) dispersion; Mortar; Properties; Curing temperature; Relative humidity (RH)

<https://doi.org/10.1631/jzus.A2000526>

**CLC number:** TU502


## 1 Introduction

Cementitious materials have been widely used in building construction all over the world (Wang et al., 2020). Traditionally, ordinary Portland cement (OPC) has been the most common choice. However, it has some shortcomings including high CO<sub>2</sub> emissions, amounting to about 0.87 t for each ton produced, and

low resistance to aggressive environments, such as conditions with high acidity or high sulfate concentrations (Ali et al., 2011; Juenger et al., 2011).

Calcium sulfoaluminate (CSA) cement shows better environmental performance (Qiu et al., 2010; Tan et al., 2020). The sintering temperature of its clinker is about 1250 °C, some 200 °C lower than that of OPC, and thus its production consumes less energy (Juenger et al., 2011). The release of CO<sub>2</sub> derives from the decarbonation of limestone or other replacement materials from a calcium source that are used in the production of OPC and CSA cement.

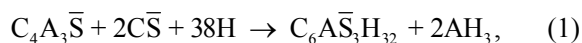
\* Project supported by the National Natural Science Foundation of China (Nos. 51872203 and 51572196)

 ORCID: Ru WANG, <https://orcid.org/0000-0002-0121-0144>

© Zhejiang University Press 2021

However, the main clinker component of CSA cement, ye'elite ( $C_4A_3\bar{S}$ ), has a lower enthalpy of formation and produces 0.36 t less  $CO_2$  per ton of clinker than the main clinker component of OPC, tricalcium silicate ( $C_3S$ ) (Sharp et al., 1999). The raw materials of CSA cement can be sourced from many waste materials, including incinerated municipal solid waste and phosphochalk (Singh et al., 2008; Shi et al., 2009). The strength of CSA cement is comparable to that of OPC and it has many other superior properties including low permeability, rapid hardening, and resistance to sulphate and chlorine erosion. This makes CSA a promising low- $CO_2$  alternative to Portland cement in some projects (Lu et al., 2009; Zhang et al., 2009; Cai and Zhao, 2016).

The main component of CSA cement is  $C_4A_3\bar{S}$  with a lower content of belite ( $C_2S$ ), anhydrite ( $C\bar{S}$ ) or gypsum ( $C\bar{S}H_2$ ) (Glasser and Zhang, 2001). The most important hydration product, ettringite ( $C_6A\bar{S}_3H_{32}$ , AFt), forms immediately when  $C_4A_3\bar{S}$  and  $C\bar{S}$  are mixed with water (Eq. (1)) (Sharp et al., 1999). Aluminium hydroxide ( $AH_3$ ) also forms during this process. In the presence of calcium hydroxide (CH), the hydration of  $C_4A_3\bar{S}$  is accelerated to form more ettringite (Eq. (2)) (Sharp et al., 1999). If the  $C\bar{S}$  is consumed completely during the hydration,  $C_4A_3\bar{S}$  will hydrate to form monosulfate ( $C_4A\bar{S}H_{12}$ , AFm) (Eq. (3)) (Liao et al., 2011). Depending on the minor phases in the CSA cement, other hydration products may be observed, such as siliceous phases (strätlingite and siliceous hydrogarnet), gehlenite, and calcium silicate hydrate (C-S-H) (Winnefeld and Lothenbach, 2010).



However, the main hydration product, AFt, makes the CSA cement matrix sensitive to temperature and ageing. The decomposition of AFt early in the hydration of CSA cement results from high temperature and a lack of gypsum (Liao et al., 2011). The pore structures of CSA cement pastes tend to be

coarsened at elevated temperatures (Zhang and Glasser, 2002). Changing the curing temperature does not change the type of hydration products, but does affect their amounts (Wang et al., 2017). Some studies (Berger et al., 2011; Wang et al., 2017) have focused on the influence of curing temperature (0–80 °C) on hydration evolution and compressive strength. Results showed that the maximum amounts of AFt and AFm appear at 20 °C and 40 °C, respectively, and that low temperatures (<20 °C) favor a denser and more homogeneous matrix due to continuous and substantial hydration. Also, Li et al. (2019) found low temperature and high humidity contribute to the formation of AFt and a reduction of cement phase porosity in CSA cement systems during the early period. AFt, the main product responsible for the strength of CSA, is quite sensitive to curing conditions, and tends to decompose to AFm at elevated temperatures. This may lead to strength reduction and degradation of hardened pastes in practical projects (Zhang and Glasser, 2002).

An innovative method often applied to OPC, which may also be suitable for modifying CSA cement, is to add polymers to cement when mixed with water. Aqueous dispersion such as styrene-butadiene copolymer (SB) dispersion, styrene-acrylic ester copolymer (SAE) dispersion, and polyacrylic ester (PAE) dispersion are the most often used polymers to cement mortar and concrete (Chung, 2004). Polymers that enhance the cement matrix can be divided into two types according to their mode of action. The first type, including SB, has no active groups and enhances the system mainly through physical modification. The polymer forms a film and fills the cracks and pores in the cement matrix. The second type, including SAE, has active groups that can react with hydration products in addition to its physical action, thus contributing to stronger adhesion and cohesion of cement mortar and concrete (Yang et al., 2009; Xu et al., 2010; Wang M et al., 2015; Wang R et al., 2016; Eren et al., 2017). Addition of polymers has four main effects in macro level (Qian and Zhan, 2002; Yang et al., 2009; Aboelkheir et al., 2018; Assaad, 2018; Han et al., 2018; Moradi et al., 2018; Kim, 2020; Shi et al., 2020): (a) improvement in workability due to their air-entrainment; (b) enhancement of mechanical properties, such as flexural strength, toughness, and ductility; (c) increased durability, such

as impermeability, and resistance to carbonation and chloride penetration; (d) other beneficial effects including water reduction and delaying setting. Several factors influencing the properties of polymer-modified cement matrix have been studied. Some studies that focused on the types of polymers showed that different polymers have totally different effects on Portland cement (Poon and Groves, 1987; Zhong and Chen, 2002). Other studies found that a polymer can exhibit two opposite effects when the dosage is changed, demonstrating the importance of choosing the optimal mixing content (Liu et al., 2003; Li et al., 2018). However, research on adding polymer to CSA cement-based material is quite limited. In our previous study, we examined the effect of three polymer dispersions (SB, SAE, and PAE) on the early hydration of CSA cement. The results showed that the addition of polymer dispersion retarded the initial hydration of CSA cement, especially within 1 h, but accelerated hydration and Aft formation after 2 h. PAE showed the most powerful acceleration effect (Li et al., 2020). The three kinds of polymer dispersion were also used to prepare mortars to study their influence on the properties of CSA cement mortar before 28 d. Results showed that polymer dispersion helps to improve microstructure by forming continuous films in CSA cement mortar, thereby enhancing its mechanical properties (flexural and tensile bond strength) and durability (resistance to carbonization, sulfate attack, and water) (Li et al., 2018). CSA cement mortar modified by SB dispersion (SBMM) showed the best properties, including improved freeze-thaw cycle resistance. The effect of curing regimes on the properties of SBMM before 28 d was studied. High temperature and high relative humidity (RH) were found to be beneficial for the formation of Aft and the early development of mechanical properties (Wang et al., 2019).

These studies indicate that the initial properties of CSA cement mortar are enhanced by adding SB dispersion. However, the long-term performance of polymer-modified CSA cement mortar is unclear. Also, there are some concerns that CSA cement specimens with free or low gypsum content have unstable properties during a long period, especially under thermal excursion (Berger et al., 2011). Therefore, it is of great significance to investigate the long-term properties of CSA cement mortar modified

by SB dispersion, to ensure its safe application. In this study, the development of properties of SB dispersion-modified CSA cement mortar, cured under different conditions, was investigated from 28 to 360 d. The morphology of mortars cured under different conditions for 360 d was studied using scanning electron microscope (SEM).

## 2 Experimental methods

### 2.1 Materials

The cement used in this experiment was 52.5 rapid hardening CSA cement. The mineralogical phases and chemical composition of the CSA cement are shown in Tables 1 and 2, respectively. A typical ECO7623 styrene-butadiene copolymer dispersion was used, with the characteristics shown in Table 3. The results of particle size analysis of CSA cement and SB dispersion are shown in Table 4 and Fig. 1. Standard sand and water used in this experiment complied with the provisions of ISO 679-2009 (ISO, 2009). The defoaming agent used in the test was Foamaster® MO NXZ mineral oil defoamer (BASF China).

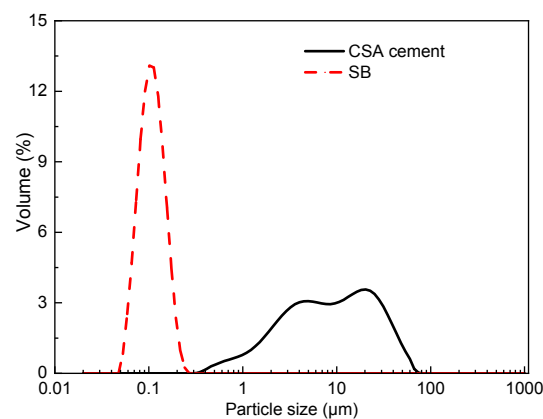


Fig. 1 Particle size distributions of CSA cement and SB

### 2.2 Mixing proportions, curing, and testing

In this study, five different polymer-to-cement ratios ( $m_p/m_c$ ) by mass (0%, 5%, 10%, 15%, and 20%) were used to prepare polymer-modified cement mortar. Silicone base defoamer of 2% was added to the SB dispersion in advance to remove air. The cement-to-sand ratio was 1:3. The water requirement was determined by keeping a constant flow, according

**Table 1 Mineralogical phases of CSA cement (unit: %) (in weight)**

$C_4A_3\bar{S}$	$C_2S$	$C\bar{S}$	$C_4AF$	$C_{12}A_7$	CT	$CaMg(CO_3)_2$	MgO	Amorphous
35.4	26.4	14.3	4.6	3.1	1.0	1.5	1.9	11.7

**Table 2 Chemical composition of CSA cement (unit: %) (in weight)**

$Al_2O_3$	CaO	$SO_3$	$SiO_2$	$Fe_2O_3$	$K_2O$	MgO	$Mn_2O_3$	$Na_2O$	$P_2O_5$	SrO	$TiO_2$	LOI
23.84	44.20	15.04	9.82	1.95	0.26	2.46	0.02	0.08	0.11	0.10	0.95	1.17

LOI: loss on ignition

**Table 3 Characteristics of SB dispersion**

Average particle size ( $\mu m$ )	pH value	Lowest film-forming temperature ( $^{\circ}C$ )	Solid content (%)	Viscosity (mPa·s)	Glass transition temperature ( $^{\circ}C$ )
0.112	7.0–9.0	15	52	35–150	14

**Table 4 Particle size distributions of CSA cement and SB**

Item	Size ( $\mu m$ )		
	D10	D50	D90
CSA cement	1.815	9.038	34.002
SB	0.076	0.112	0.168

to the flow table value of GB/T 2419-2005 (GAQSIQ, 2005). The water-to-cement ratio ( $m_w/m_c$ ), containing the water in SB dispersion, was adjusted to make sure the flow table value at  $(175\pm 5)$  mm.

The SB dispersion was first weighed into tap water and then the specific amount of CSA cement was blended into the liquid to prepare the fresh mortar according to ISO 679-2009 (ISO, 2009).

The mortar specimens for testing flexural and compressive strength were prepared by casting the fresh mortar mixtures into 40 mm×40 mm×160 mm prismatic molds, which were then compacted with an external vibrator according to ISO 679-2009 (ISO, 2009). The molds containing the mortar specimens were then immediately placed in curing chambers at various temperatures and RH values for initial curing. After 24 h, all specimens were demolded and transferred to the chambers again for further curing. In this study, the curing regimes covered five temperatures (0, 5, 10, 20, and 40  $^{\circ}C$ ) and three RHs (low, middle, and high). The temperature was controlled using an environmental chamber, and different RH values were achieved using saturated salt solution according to ASTM E104-02 (ASTM, 2002). Low RH (LRH) was achieved using magnesium chloride ( $MgCl_2$ ) saturated

solution, middle RH (MRH) using sodium bromide ( $NaBr$ ), and high RH (HRH) using potassium sulfate ( $K_2SO_4$ ) saturated solution. The RHs of the  $MgCl_2$ ,  $NaBr$ , and  $K_2SO_4$  saturated solutions were calibrated with an Extech RH10 humidity and temperature USB datalogger. The LRH ranged from 31.6% to 33.6%, the MRH ranged from 53.2% to 63.5%, and the HRH ranged from 96.4% to 98.5%. The flexural and compressive strength values after 28, 56, 90, 180, and 360 d were tested according to the ISO 679-2009 (ISO, 2009). The flexural and compressive strength estimates obtained were the average of three and six values, respectively.

The specimens for testing tensile bond strength were prepared according to JC/T 985-2005 (CBMC, 2005). Molds of 50 mm×50 mm×5 mm were placed on a concrete board, then fresh mixtures were cast in the molds to prepare the specimens. The specimens and concrete board were placed in the curing chambers at various temperatures and RH values for 24 h, then demolded and returned to the chambers for subsequent curing. The tensile bond strength was tested when the specimens were aged 28, 56, 90, 180 or 360 d. Before the day of measurement, the specimens were taken out of the curing chamber and glued to an iron block using epoxy resin. The specimens were then placed in the chamber again to complete the curing. Testing was performed following the standard JC/T 985-2005. The tensile bond strength estimate was an average of eight values.

The procedure for preparing specimens for water capillary absorption (WCA) testing was the same as

that of preparing the flexural and compressive strength specimens. The testing of WCA was carried out following ISO 15148-2002 (ISO, 2002). After 28, 180 or 360 d of curing in various curing regimes, specimens were dried at 60 °C for 48 h and then the four sides were sealed with paraffin. Afterwards, the upside of each specimen was immersed in water. The WCA, expressed in terms of water absorption per unit area at 48 h, was an average of three values.

The microstructure of the specimens was analyzed using SEM as follows. The initial samples, cured for 360 d at different temperatures and RHs, were crushed into pieces and some pieces with a relatively complete plane of about 1 cm<sup>2</sup> were chosen as the final samples. All reference mortar (RM) and SBMM samples were then soaked in alcohol, and the alcohol was replaced every two days. After one week, the samples were taken out of the alcohol and dried in an oven at 50 °C until completely dry. Finally, the samples were coated with gold and observed using SEM.

### 3 Results and discussion

#### 3.1 Flexural strength

##### 3.1.1 Reference mortar

The mortar of specimens without SB dispersion was denoted as RM. Fig. 2 shows the variation of the flexural strength of RM with age at different temperatures and RH values. Under all curing conditions, the flexural strength of RM increased first and then decreased with increasing curing time. When cured at LRH and temperatures of 0, 5, 10 or 20 °C, the flexural strength of RM kept increasing in the first 90 d, especially from 28 to 56 d, and then declined till 360 d. The flexural strength of RM cured at 40 °C reached the maximum at 56 d, and then declined until 360 d, especially from 56 to 90 d. When cured at MRH, the flexural strength of RM at 0, 5 or 10 °C increased up to 90 d then started to decrease, whereas at 20 or 40 °C, the maximum flexural strength was achieved at 56 d. When cured at HRH, the flexural strength of RM first increased at all curing temperatures, then declined after reaching a maximum at 56 d or 90 d. Clearly, the flexural strength of RM was seriously reduced following a long curing time at all

curing temperatures and RH values. The principal reason is that the main product of CSA cement, Aft, has transformed (Peng et al., 2006) during prolonged curing, which causes volume change leading to a change in pore structure.

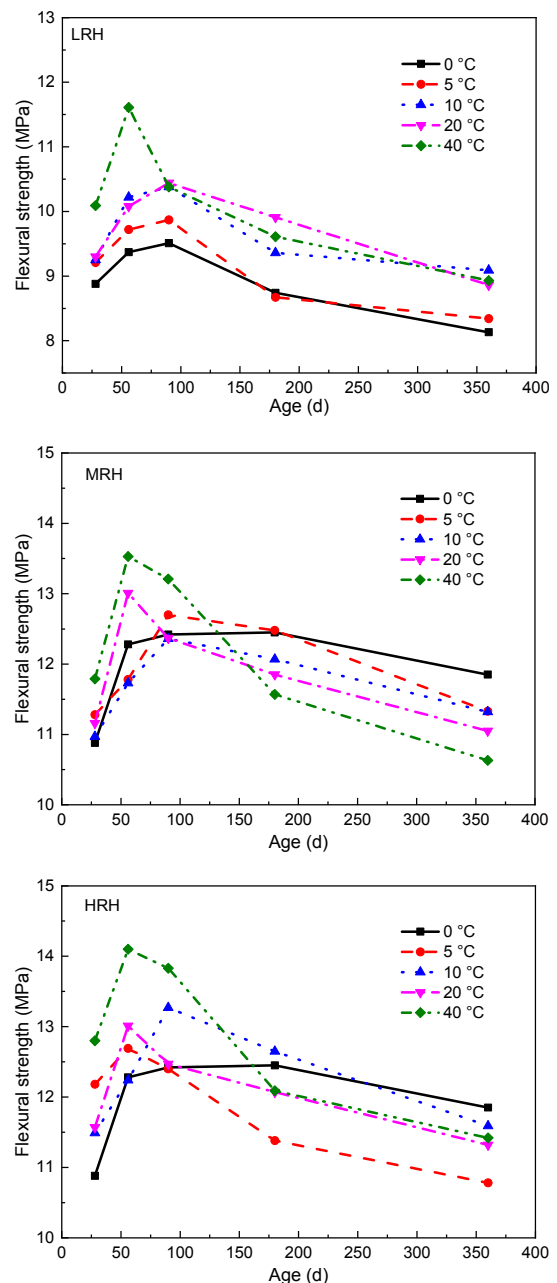


**Fig. 2 Flexural strength development of RM at different temperatures and RHs**

Note that at 0 °C and LRH the reduction in flexural strength was much more serious than at MRH

and HRH. Mortar cured at 0 °C had the lowest flexural strength at LRH, but when the RH rose to MRH or HRH, mortar cured at 0 °C showed the highest flexural strength at 360 d. The probable reason is that when mortar is cured at LRH, a large amount of moisture is lost into the air even at 0 °C, but when the RH rises to MRH or HRH, mortar cured at 0 °C suffers less moisture loss compared with mortars cured at higher temperatures. Thus, at 0 °C the strength can

develop slowly and shows less reduction at a later age. This indicates that the effects of temperature and humidity on the flexural strength of long-term CSA cement mortar are complicated and need further research.

### 3.1.2 Effect of SB dispersion

Fig. 3 shows the relationship between the flexural strength and the age of SBMM at different

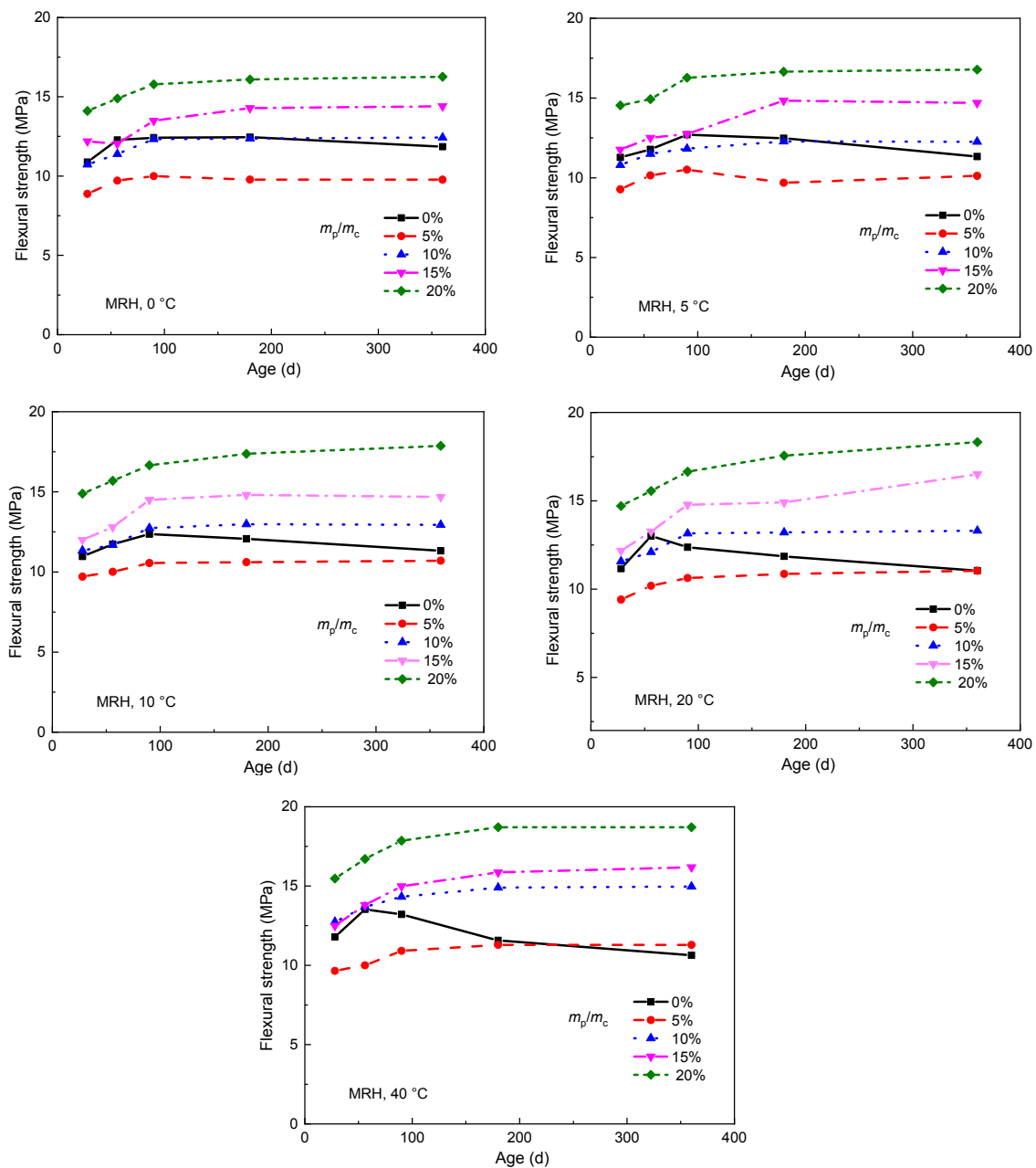
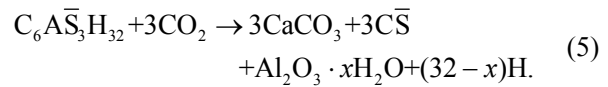
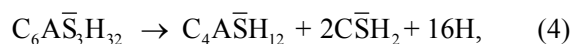


Fig. 3 Effect of SB content ( $m_p/m_c$ ) on the flexural strength development of CSA cement mortars cured at MRH and different temperatures

temperatures at MRH. The flexural strength of SBMM kept increasing during the curing period and increased with the rise in SB content. Addition of SB dispersion to CSA cement mortar created two beneficial macro-effects. One was to promote high growth in flexural strength with the addition of over 10% SB. The flexural strength of SBMM with 20% SB at 360 d was at least 50% higher than that of RM. The other was to restrict the reduction in strength in the later period, as shown by minimal change in flexural strength between 180 and 360 d in all SBMM groups. Note that when SB was added at 5%, the flexural strength of SBMM at 360 d was lower than that of RM at low temperatures (0, 5, and 10 °C), but was equal to that of RM at 20 °C, and higher than that of RM at 40 °C. The development trend of the flexural strength of SBMM at LRH and HRH was similar to that at MRH.

As discussed above, polymer dispersion enhances toughness. However, addition of polymer dispersion also has the negative effect of introducing more voids as a result of air entrainment, although this effect can be restricted to some extent by using a defoamer (Wang et al., 2019). These positive and negative effects oppose each other. When 5% SB is added, there is not enough polymer to form a continuous film structure to connect the hydration products and fill in the introduced voids, thus bringing about a reduction in flexural strength. When the SB addition reaches 10% or more, a more continuous polymer film is formed to enhance the “bonding bridge” effect and fill in the voids, so the flexural strength is strengthened.

The reduction in strength of CSA cement mortar may derive from two causes. First, AFt easily decomposes into AFm at high temperature and low humidity, according to Eq. (4) (Mehta, 1972; Barbarulo et al., 2005). Second, AFt tends to be carbonized by CO<sub>2</sub> in the air after prolonged curing, according to Eq. (5) (Nishikawa et al., 1992). These two reactions result in a decrease of AFt and a deterioration of mortar structure. The alleviation of the strength reduction by SB dispersion after prolonged curing may result from the formation of a polymer film in the SBMM that can prevent the transformation and carbonation of AFt.



### 3.1.3 Effect of temperature

Fig. 4 shows the flexural strength development of RM and SBMM cured at MRH and different temperatures. It is clear that high temperature is beneficial to the flexural strength development of RM before 90 d. However, increasing temperature aggravates the decline of flexural strength of RM after 90 d, indicating that low temperature is more suitable for the development of flexural strength in consideration of long-term performance. The development of flexural strength of SBMM differed from that of RM. The flexural strength of SBMM in most groups increased as the curing temperature increased, indicating that high temperature is conducive to the development of the flexural strength of SBMM. The effect of temperature on the flexural strength of SBMM at LRH and HRH was similar to that at MRH. The probable reason is that high temperature is inclined to promote the formation of a complete polymer film (Beeldens et al., 2005; Wang et al., 2019), which is an important factor affecting the flexural strength. In summary, high temperature and high polymer content are conducive to high flexural strength. However, the effect of temperature is not as significant as the effect of polymer content.

### 3.1.4 Effect of relative humidity

Fig. 5 (p.1013) shows the flexural strength of RM and SBMM cured at 20 °C and different RH values. The higher the humidity, the higher the flexural strength of all mortars. When the RH increased from LRH to MRH, the flexural strength of all the mortars, regardless of their curing age or SB content, increased significantly. When the RH increased from MRH to HRH, the flexural strength of RM hardly changed; however, this increase in RH greatly increased the flexural strength of SBMM. At LRH, MRH, and HRH, the flexural strength of RM reached the maximum at 90, 56, and 56 d, respectively, which indicates that the increase of RH is conducive to the early development of flexural strength of RM. The impact of RH on the flexural strength of all mortars cured at 0, 5, 10 or 40 °C was similar to that at 20 °C, and so is not discussed further here.

### 3.2 Compressive strength

#### 3.2.1 Reference mortar

The change of compressive strength of RM with age at different temperatures and RH values is shown in Fig. 6 (p.1014). The compressive strength of RM first increased and then decreased till 360 d as the curing age increased under all conditions except HRH/40 °C, which showed a high compressive strength at 28 d and then a decrease till 360 d. We

can conclude that higher temperatures and RH are conducive to achieving faster early compressive strength development, but tend to advance the start of the subsequent reduction and lead to a lower compressive strength value after reduction. For example, RM cured at 0 °C and LRH reached its highest compressive strength at 90 d, but the period was shortened to 28 d when the temperature was increased to 40 °C and the RH increased to HRH. However, high temperature was not beneficial to later compressive

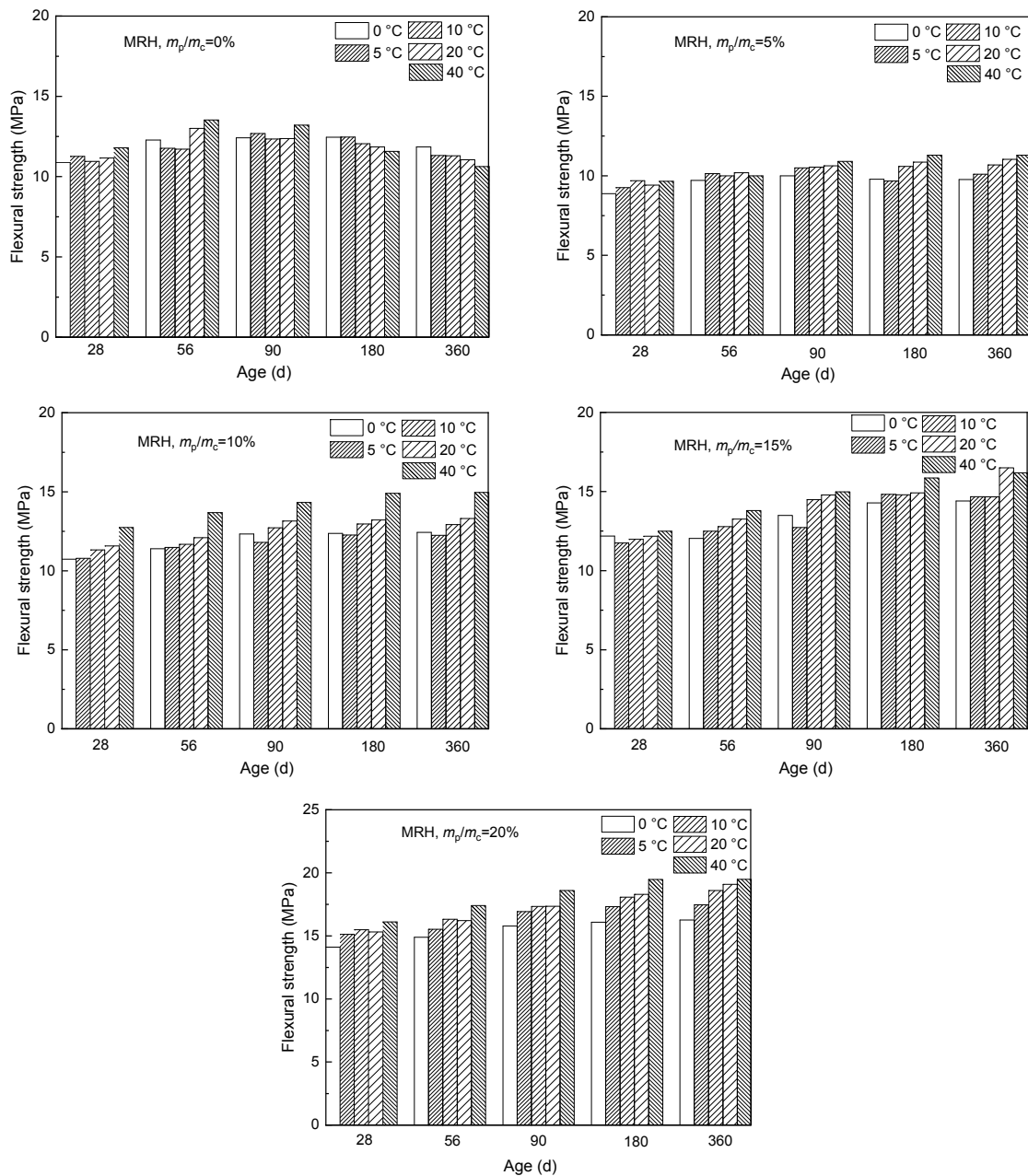


Fig. 4 Effect of temperature on the flexural strength development of RM and SBMM cured at MRH



strength development. The finding that RM at 360 d, regardless of the RH value, attained the highest compressive strength when cured at 10 °C proves the point. Meanwhile, RM at all curing temperatures and RH values showed a severe reduction in compressive strength, ranging from 5.4% to 19.0%, resulting from the transformation of AFt into AFm. This transformation results from the change in the concentration of ions in the paste following hydration of the cement (Peng et al., 2006; Wang XB et al., 2016).

The effects of the temperature and humidity on compressive strength at 360 d were different from those on flexural strength. This may be related to effects on hydration and microstructure, and is worthy of further investigation.

### 3.2.2 Effect of SB dispersion

The effect of SB content on the compressive strength development of CSA cement mortar cured at MRH and different temperatures is shown in Fig. 7

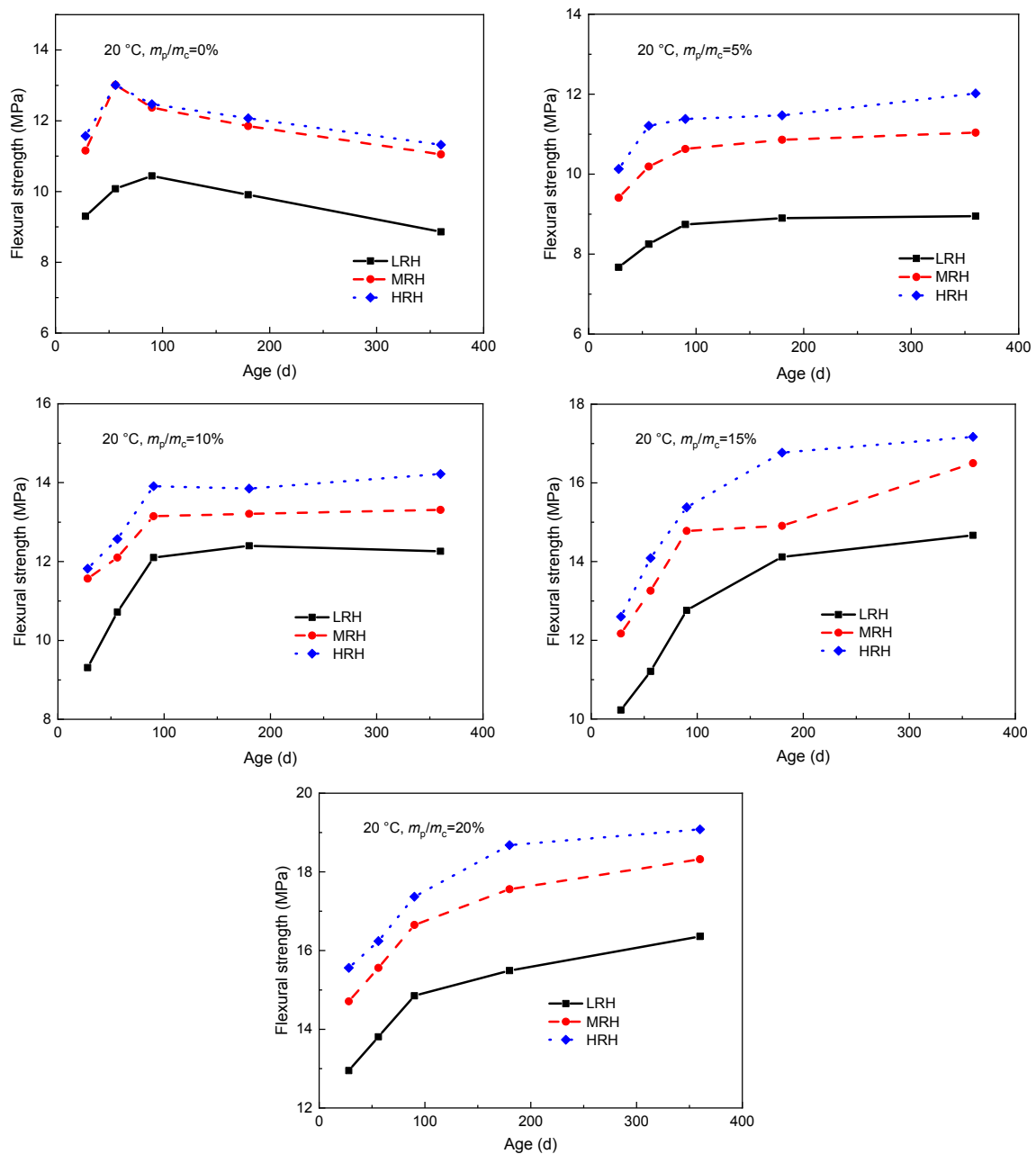
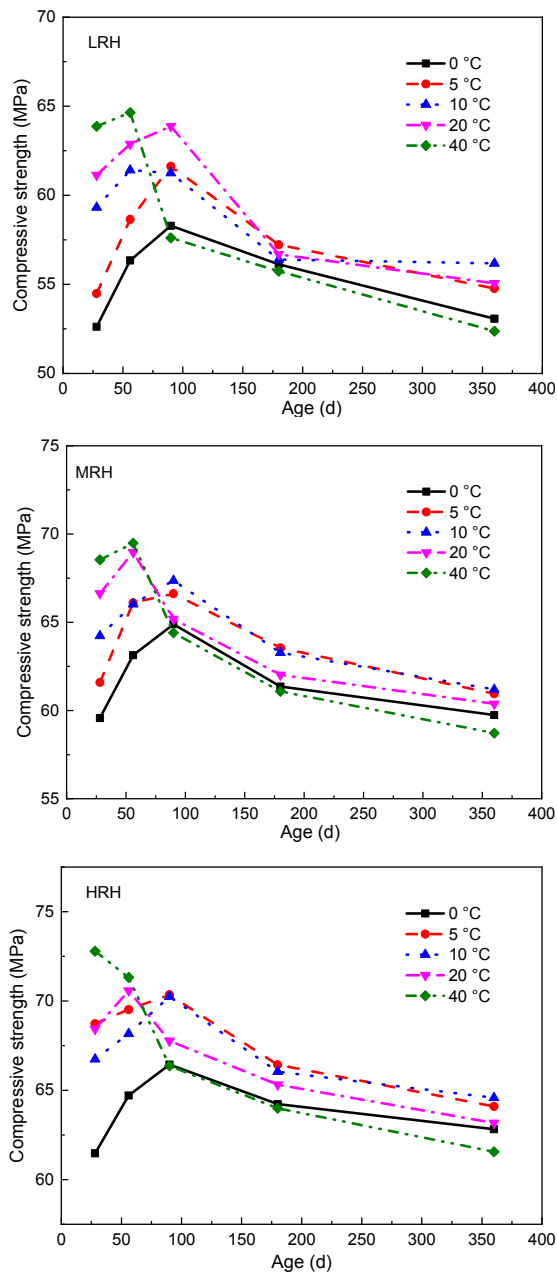


Fig. 5 Effect of RH on the flexural strength development of RM and SBMM cured at 20 °C



**Fig. 6 Compressive strength development of RM under different temperatures and RHs**

(p.1015). The trend of the compressive strength of all SBMMs was similar, i.e. the compressive strength increased with age up to 180 d, and at 360 d was roughly the same as that at 180 d. The compressive strength of SBMM increased with increasing SB content. This increase was significant when the mixing content increased from 5% to 10%. However, when the content of SB exceeded 10%, the increase in compressive strength of the modified mortar was

weakened. It is apparent that SBMM had a lower compressive strength than RM even when the strength of RM had already been reduced, but increasing temperature narrowed the difference in compressive strength between SBMM and RM. For example, at 0 °C, the compressive strength of SBMM with 20% SB content was 80% of that of RM, but when the temperature rose to 40 °C, their compressive strength values were almost the same. The development trends of compressive strength of SBMM at LRH and HRH were similar to those at MRH.

A polymer is a kind of flexible filler that can form a film between hydrated products, thereby enhancing their toughness (Cao et al., 2012, 2013) and preventing strength reduction of a cement matrix. As discussed above, the addition of polymer had a negative effect on the development of compressive strength. The reason is probably that the addition of SB dispersion introduced more voids in the mortar matrix, most of which were filled later by the polymer film (Section 3.5). The enhancement of toughness by a polymer filling voids and bonding hydration products is directly related to the situation where the mortar is subjected to bending and tensile stresses. However, when mortar with SB is subjected to compressive stress, the pressure affects every part of the mortar. The compressive strength of the flexible polymer is not as high as that of the hydration products. Therefore, the SB contributes to only the flexural strength, not the compressive strength.

### 3.2.3 Effect of temperature

Fig. 8 (p.1016) shows the compressive strength development of RM and SBMM cured at MRH and different temperatures. High temperature promoted early strength development of RM, as shown by the data of 28 d. However, once compressive strength reduction of RM started, the decline was more significant at higher curing temperatures. This trend was similar to that of flexural strength development. RM cured at 10 °C had the highest compressive strength in the later period and good compressive strength in the early period, suggesting that a proper curing temperature contributes to the development of both early and later strengths. The compressive strength of SBMM increased with the rise of curing temperature at any curing age. The development trends of the compressive strength of mortars cured at LRH and

HRH were similar to those cured at MRH. The main reason is that at high curing temperatures the formed polymer film can interweave tightly with the hydration products of CSA cement to produce a stronger network structure (Beeldens et al., 2005; Wang et al., 2019).

### 3.2.4 Effect of relative humidity

Fig. 9 (p.1017) shows the compressive strengths of RM and SBMM at 20 °C and different RH values.

The compressive strengths of all mortars increased with increasing RH. The difference of compressive strength between mortars cured at LRH and MRH was significantly greater than that between mortars cured at MRH and HRH. For RM, the maximum compressive strength under curing at LRH occurred at 90 d, while for mortars cured at MRH and HRH the maximum compressive strength occurred at 56 d. This phenomenon also demonstrates that elevating RH is beneficial to early compressive strength

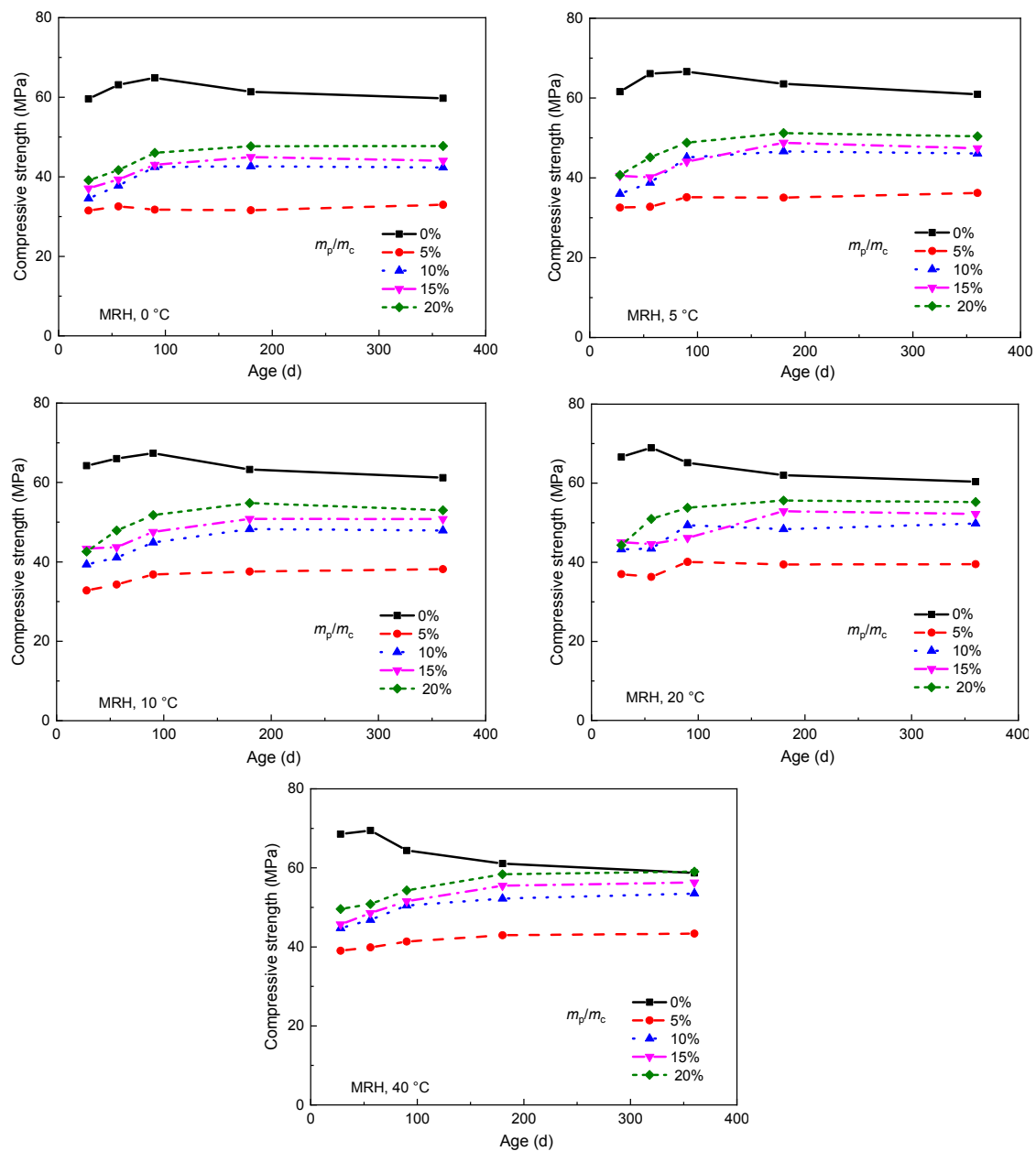


Fig. 7 Effect of SB content ( $m_p/m_c$ ) on the compressive strength development of CSA cement mortars cured at MRH and different temperatures

development. The effect of humidity on the compressive strength of all mortars cured at 0, 5, 10 or 40 °C was similar to that at 20 °C, and so is not discussed further here.

### 3.3 Tensile bond strength

#### 3.3.1 Reference mortar

Fig. 10 (p.1018) shows the tensile bond strength of RM cured at different temperatures and RH values.

When cured at 0 °C, the tensile bond strength of RM increased up to 180 d and then started to decrease. At a curing temperature of 5 or 10 °C, all groups reached their maximum strength at 90 or 180 d. When the curing temperature was raised to 20 or 40 °C, most mortars reached their maximum tensile bond strength before 56 d. This shows clearly that high temperature is conducive to early tensile bond strength development, but induces more serious strength reduction after prolonged curing.

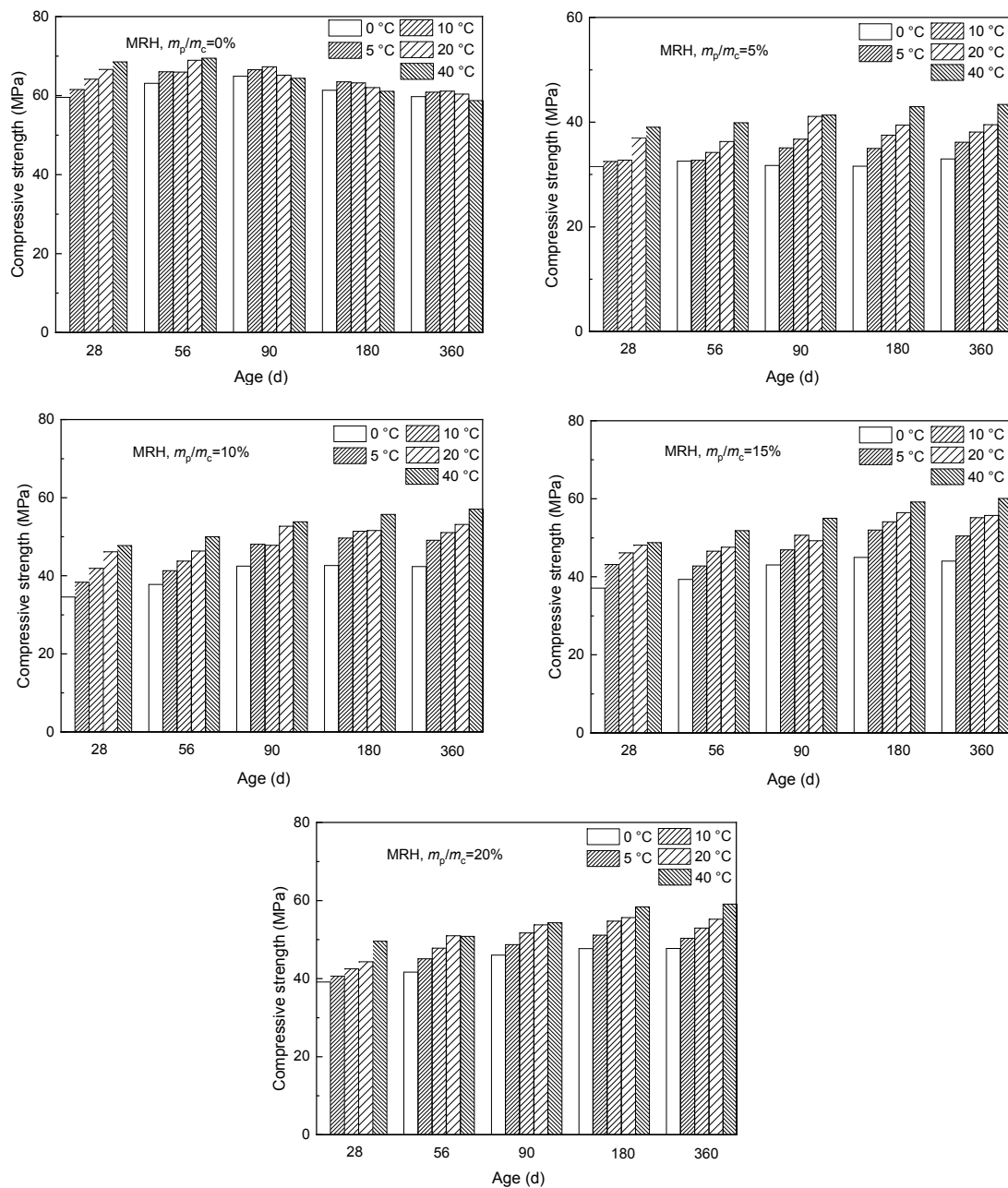


Fig. 8 Effect of temperature on the compressive strength development of RM and SBMM cured at MRH

High temperature and humidity are beneficial to the development of tensile bond strength, but the difference between the tensile bond strength caused by temperature and humidity decreases with the extension of curing age. For example, when cured at HRH for 28 d, the tensile bond strength of RM at 0, 5, 10, 20, and 40 °C was 1.57, 1.66, 1.85, 2.09, and 2.14 MPa, respectively. Thus, the difference between the highest and the lowest values was 0.57 MPa. However, when the curing age reached 360 d, the

tensile bond strength of RM at 0, 5, 10, 20, and 40 °C was 1.69, 1.77, 1.83, 1.88, and 1.97 MPa, respectively, and the difference between the highest and the lowest values was only 0.28 MPa. When cured at 20 °C for 28 d, the tensile bond strength of RM at LRH, MRH, and HRH was 1.81, 1.90, and 2.09 MPa, respectively, with a difference of 0.28 MPa. However, when cured at 20 °C for 360 d, the tensile bond strength of RM at LRH, MRH, and HRH was 1.73, 1.77, and 1.88 MPa, respectively, with a difference of

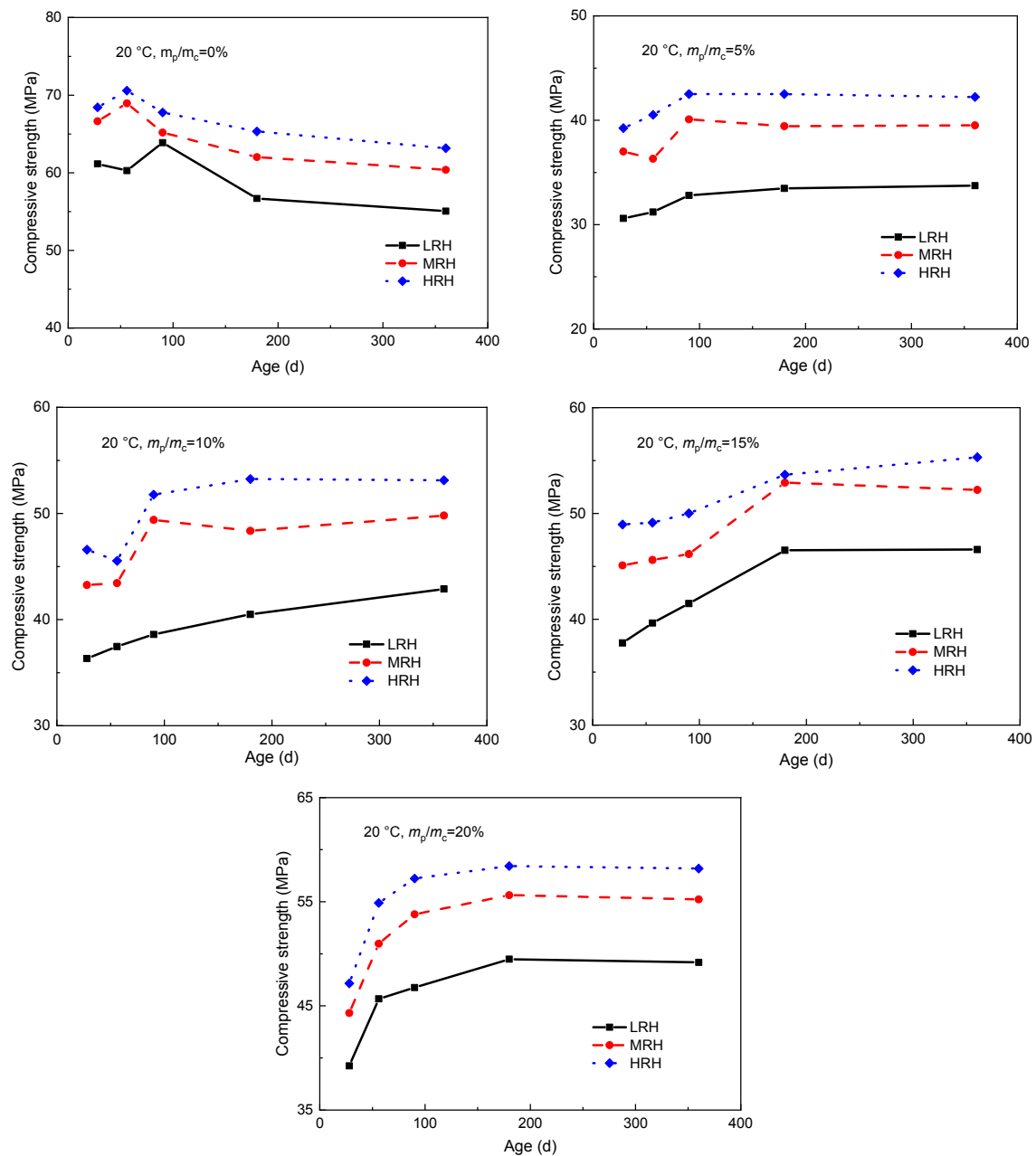
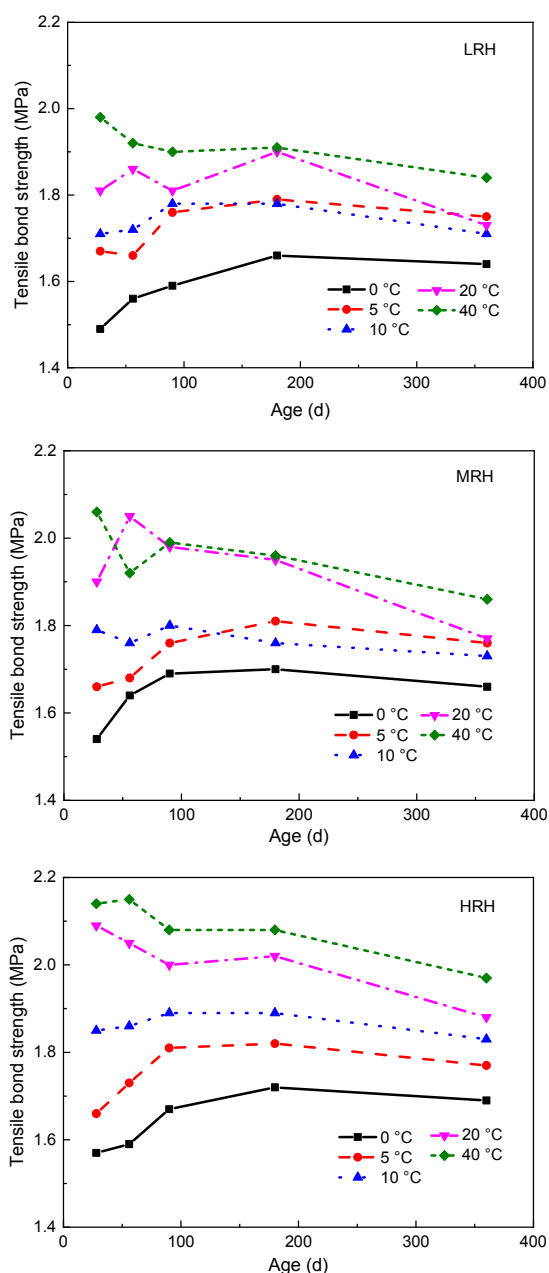


Fig. 9 Effect of RH on the compressive strength development of RM and SBMM cured at 20 °C

only 0.15 MPa. This phenomenon is probably due to the hydration of CSA cement, which was almost complete in the later period among all groups, but varied greatly at the beginning under different curing regimes.

### 3.3.2 Effect of SB dispersion

Fig. 11 shows the tensile bond strength development of RM and SBMM cured at MRH and



**Fig. 10** Tensile bond strength development of RM cured at different temperatures and RHs

different temperatures. The tensile bond strength of SBMM increased steadily up to 180 d, and at 360 d was almost the same as that at 180 d. Therefore, the presence of SB can efficiently prevent the reduction of tensile bond strength. The tensile bond strength of SBMM was higher than that of RM under all curing conditions, and the higher the content of SB, the greater the tensile bond strength. Taking the data at a curing temperature of 20 °C as an example, the tensile bond strength of RM at 360 d was 1.77 MPa, whereas the tensile bond strength of SBMM was 29% higher (2.28 MPa) when blended with 10% SB, and 64% higher (2.90 MPa) when blended with 20% SB. The development trend of tensile bond strength of SBMM at LRH and HRH was similar to that at MRH.

The tensile bond strength of SBMM was also influenced by the temperature and humidity. It increased with increasing curing temperature, similar to RM, but the effect of temperature was still significant up to 360 d (Fig. 12) (p.1020). Fig. 13 (p.1020) shows the tensile bond strength development of SBMM at 20 °C and different RH values. A high RH improved the tensile bond strength development of the modified mortars. The trends of tensile bond strength development of SBMM caused by the temperature and RH were the same under other curing conditions.

### 3.4 Water capillary absorption

The WCA of RM and SBMM cured at different temperatures and RH values for various times is shown in Fig. 14 (p.1021). The addition of 5% SB slightly increased the WCA of CSA cement mortar, but the addition of more than 10% SB significantly reduced the WCA, and the higher the content of SB, the more significant the effect. When the content of SB reached 20%, the WCA of SBMM was only about one third of that of RM. This was because the filling effect of the polymer film helps to reduce the porosity and pore size, thus hindering the migration of water and causing the decline of WCA (Ramli et al., 2013).

The WCA of mortar cured at 40 °C was 2–3 times higher than that of mortar cured at 0 °C for both RM and SBMM, indicating that higher temperature curing gives a higher WCA. This is probably because the increase of temperature accelerates free water evaporation from the surface, creating more voids, and thereby providing more access to the mortar's inner open pores for the water. However, the effect

caused by the curing temperature gradually weakened with increasing SB content, indicating that SB can prevent free water evaporation at high temperatures. For both RM and SBMM, an increase of RH reduced the WCA, but the effect of RH was relatively weak compared with the effect of temperature. The reduction of WCA with RH occurred mainly because high humidity prevents free water evaporation to some extent, and at the same time may enable better

development of mortar hydration. There was very little change in WCA with curing time from 28 d to 360 d.

### 3.5 SEM analysis

#### 3.5.1 Reference mortar

SEM images of RM cured under different conditions at 360 d are shown in Fig. 15 (p.1022), in which the main hydration products, Aft and  $AH_3$ , are marked.

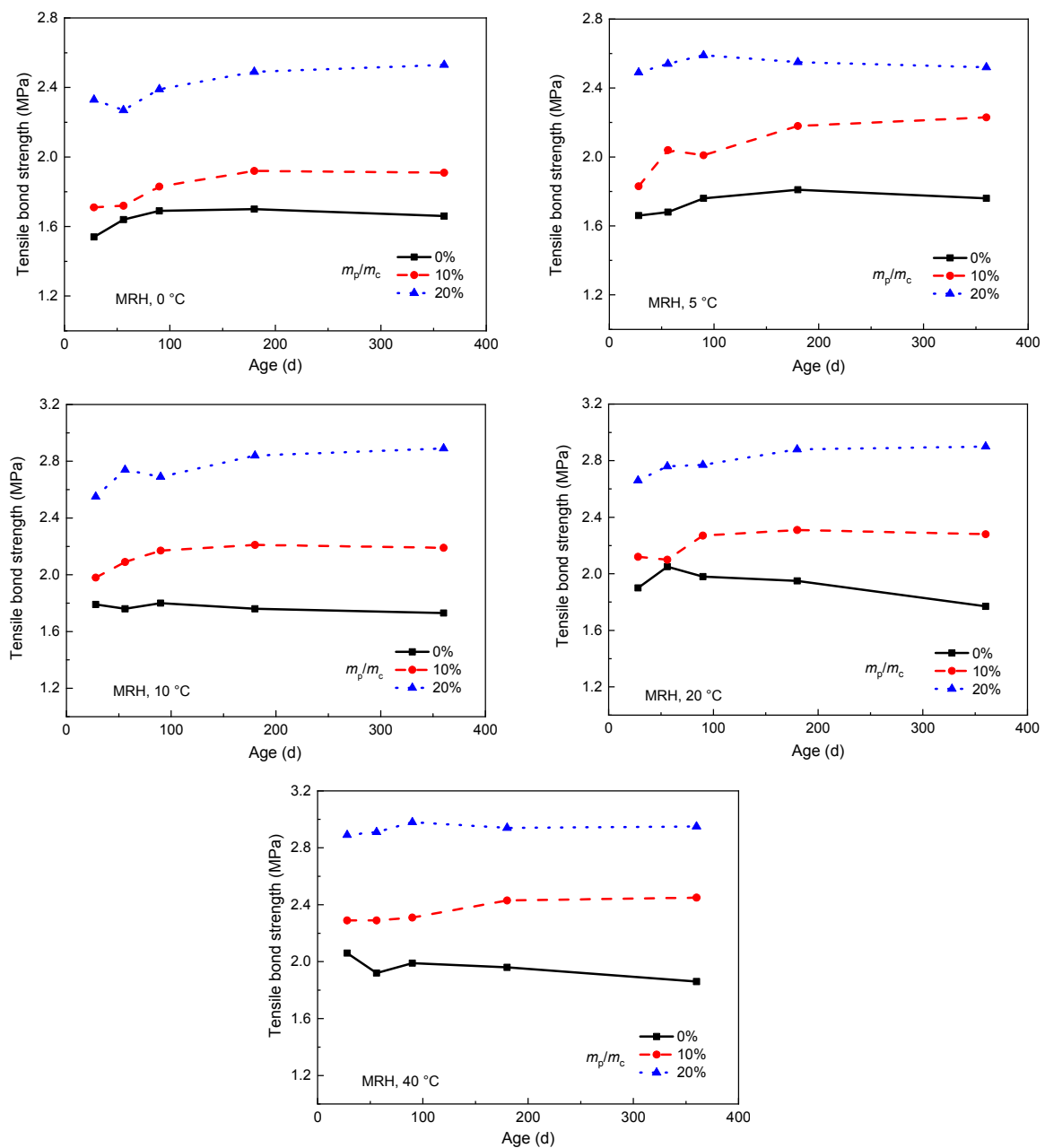
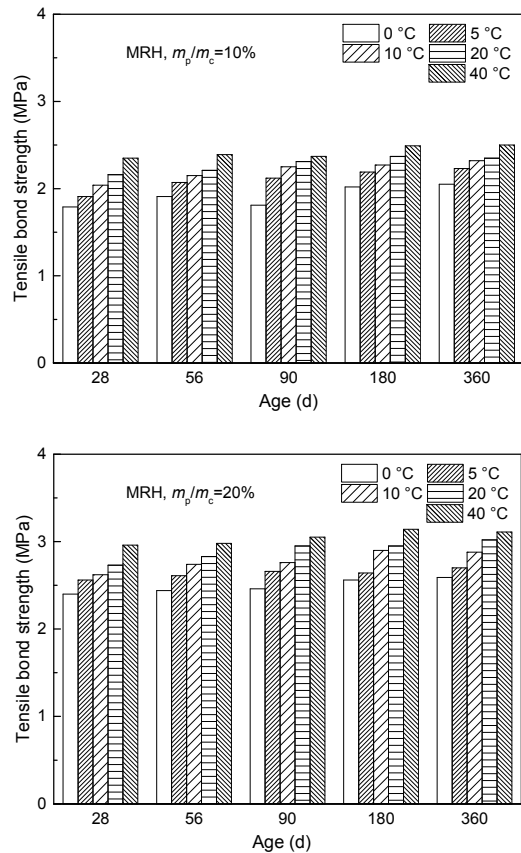
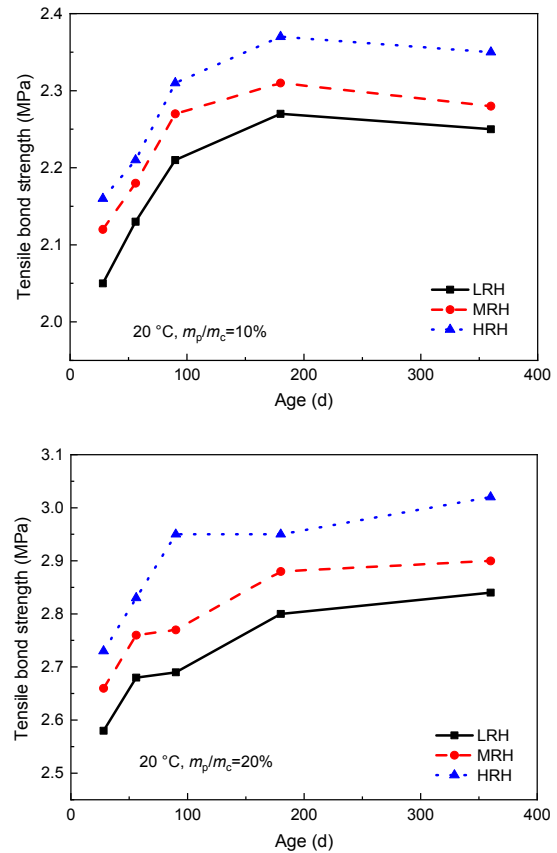


Fig. 11 Effect of SB content ( $m_p/m_c$ ) on the tensile bond strength development of CSA cement mortars cured at MRH and different temperatures



**Fig. 12** Tensile bond strength development of SBMMs cured at MRH and different temperatures

In Figs. 15a, 15d, and 15g, at 0 °C, AFt appears mainly in the form of many large needle-like elements (especially in Fig. 15g).  $\text{AH}_3$  is present as large, intact, but fewer elements. These two products are interlaced well. When the temperature increased to 20 °C (Figs. 15b, 15e, and 15h), AFt was present as fewer, smaller, flake or rodlet structures compared with the images at 0 °C. The amount of  $\text{AH}_3$  tended to increase and was no longer intact, appearing in the form of many small pieces. The AFt and  $\text{AH}_3$  were not combined tightly. When the temperature increased to 40 °C (Figs. 15c, 15f, and 15i), AFt changed to a short-column shape, but the number of AFt did not decline markedly compared with that in images at 20 °C. The number of  $\text{AH}_3$  showed a further increase. The combination of AFt and  $\text{AH}_3$  also showed deterioration compared with the images at 0 °C. The effect of a change of RH on the morphology of RM was not as obvious as the effect of a change of temperature. Usually, AFt at HRH was thinner,



**Fig. 13** Effect of RH on the tensile bond strength development of SBMMs at 20 °C

longer, and more prevalent than at LRH. This phenomenon was more obvious at 0 °C (Figs. 15a, 15d, and 15g).

To sum up, higher temperature did not benefit the preservation of AFt after prolonged curing, causing a reduction in the amount of AFt and a change in microscopic shape. At the same time, the rise of temperature led to smaller-sized, but larger amounts of  $\text{AH}_3$ . A rise of RH promoted the formation of the main hydration products, but the effect was not as significant as that of temperature. The SEM images explained well some of the macro properties, as discussed above: (1) the tensile bond strength of RM increased with the rise of temperature, which may have been due to the increased amount of  $\text{AH}_3$ ; (2) RM cured at 40 °C and 20 °C usually showed earlier strength reduction. RM may have had a faster hydration rate and smaller hydration products when cured at higher temperature, thus advancing the timing of strength reduction.



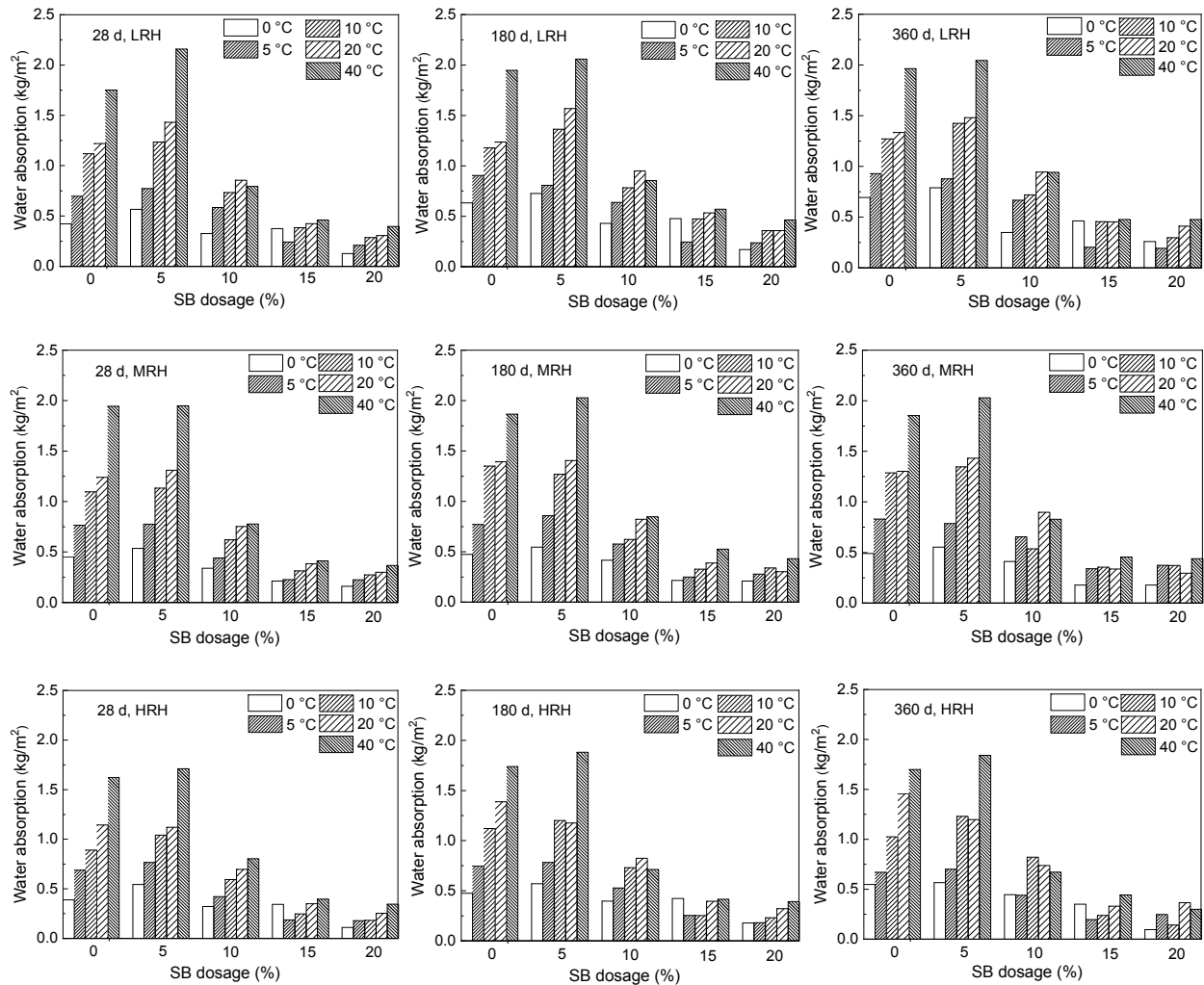


Fig. 14 WCA of SBMMs at different temperatures and RHs

### 3.5.2 Effect of SB dispersion

The SEM images of SBMM with 20% SB cured under different conditions at 360 d are shown in Fig. 16 (p.1023), in which the main hydration product, AFt is marked. Comparing Fig. 16 with Fig. 15, the hydration product AFt could not be easily found when the amount of SB increased from 0% to 20%. According to our previous research, SB retards the hydration of CSA cement and the formation of hydration products only in the first 3 h, and more AFt is formed after 3 h in SBMM than in RM (Li and Wang, 2021). From the mechanical strength data in this paper, the addition of SB dispersion can prevent the reduction in strength following long-term curing, which means that AFt can be preserved better in SBMM. Therefore,

the amount of AFt observed in SBMM was reduced probably because the AFt was covered by a polymer film. The structure of different specimens shown in Fig. 16 was always denser than that shown in Fig. 15 because of the formation of a polymer film.

The glass transition temperature of SB dispersion is 14 °C. When the temperature is below 14 °C, the polymer film is in a rigid glassy state that deforms very little under the action of external forces, thereby strongly restricting the growth and development of AFt. When the temperature is higher than 14 °C, the polymer film is in a highly elastic state that is easier to deform. AFt was invisible when the mortars were cured at 0 °C (Figs. 16a, 16d, and 16g). This is because the rigid polymer film restricts the development

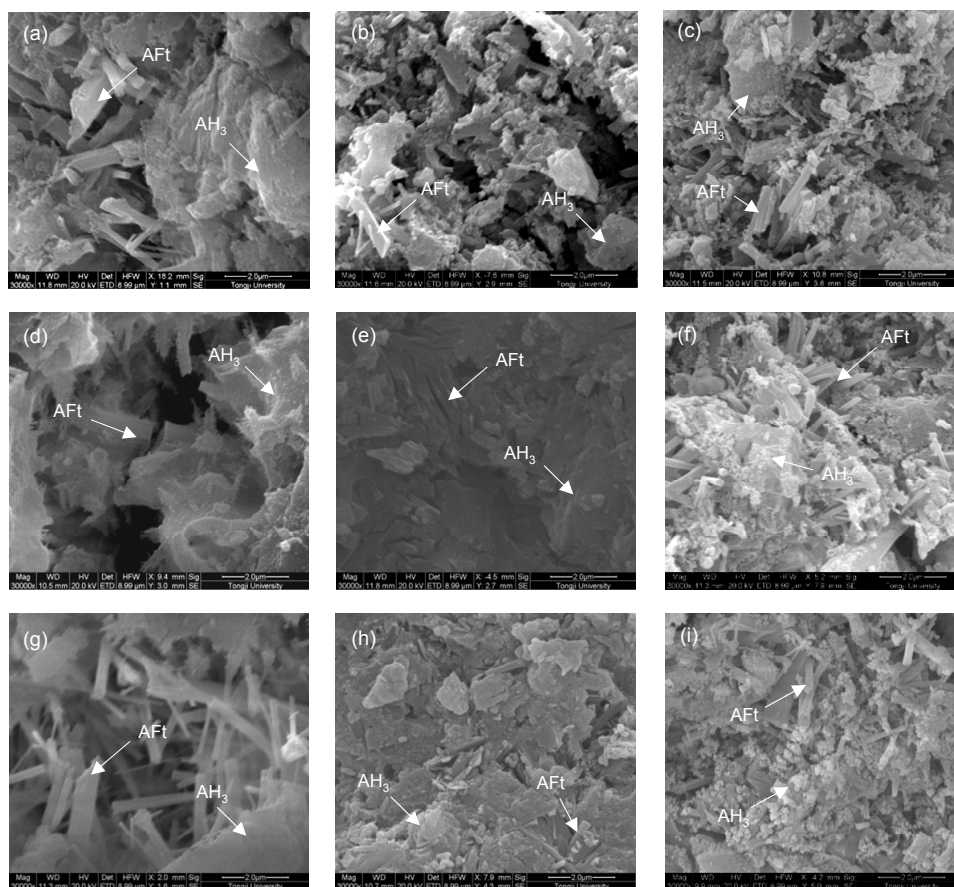


**Fig. 15** SEM images of RM cured at different temperatures and RHs at 360 d: (a) 0 °C and LRH; (b) 20 °C and LRH; (c) 40 °C and LRH; (d) 0 °C and MRH; (e) 20 °C and MRH; (f) 40 °C and MRH; (g) 0 °C and HRH; (h) 20 °C and HRH; (i) 40 °C and HRH

and growth of AFt. When the curing temperature is raised to 20 °C, the polymer film is in a highly elastic state and the restriction of AFt is weakened. AFt can grow better and be observed, and makes the polymer film become uneven (Figs. 16b, 16e, and 16h). When the curing temperature is increased to 40 °C, more AFt develops, as observed in Figs. 16c, 16f, and 16i, because the restriction effect of the polymer film is further weakened, thereby making the polymer film more uneven. The effect of a change of humidity on the morphology of SBMM was not as obvious as the effect of a change of temperature. However, comparison of images of mortars prepared at different humidities showed that AFt was more prevalent when the mortars were cured at HRH.

As discussed above, higher temperature and humidity are recommended when SBMM is cured. Based on the experimental results, the mechanical strength of SBMM cured under higher temperature

and RH is higher. However, the degree of compactness of each mortar in Fig. 16 is not significantly different because the amount of SB in each mortar is the same, and the polymer film tends to form completely at 360 d under all curing regimes.

## 4 Conclusions

1. The flexural, compressive, and tensile bond strengths of RM increase first and reach a maximum at a certain curing age, then show a reduction with the extension of curing up to 360 d. In contrast, these strengths of SBMM show a continuous increase with curing age. Reductions in all forms of strength of CSA cement mortar with age are restricted by SB dispersion.

2. The tensile bond strength grows continuously as SB content increases, whereas only more than 10%

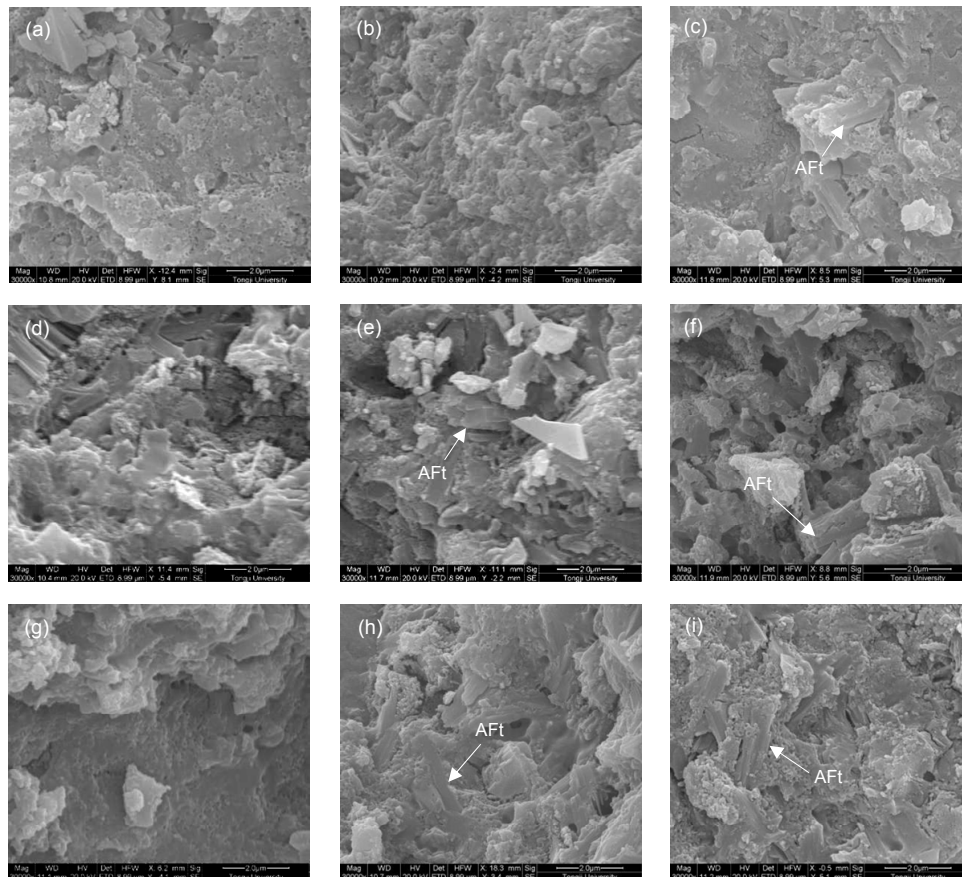


**Fig. 16** SEM images of SBMMs cured at different temperatures and RHs at 360 d: (a) 0 °C and LRH; (b) 20 °C and LRH; (c) 40 °C and LRH; (d) 0 °C and MRH; (e) 20 °C and MRH; (f) 40 °C and MRH; (g) 0 °C and HRH; (h) 20 °C and HRH; (i) 40 °C and HRH

SB addition is beneficial to the development of flexural strength, compressive strength, and waterproofness.

3. Temperature has different effects on the performance development of RM and SBMM. In RM, higher temperature favors the growth of tensile bond strength in the early stages of curing, but causes serious reductions in the flexural and compressive strengths after prolonged curing. However, in SBMM higher temperature is beneficial to all strength development. The WCA of both RM and SBMM increases with increasing temperature.

4. Higher RH is conducive to the improvement of all properties of all mortars.

5. SEM observations of RM showed that higher temperature will reduce the amount of AFt and change its microscopic shape, but will lead to the formation of more and smaller  $AH_3$ . An increase of RH can promote the formation of the main hydration products. SEM images of SBMMs showed that the

morphology of SBMM is denser than that of RM, and AFt is more visible at higher temperatures and RHs.

### Contributors

Ru WANG designed the research. Yu-sheng FAN and Tao ZHANG processed the corresponding data. Yu-sheng FAN and Ru WANG wrote the first draft of the manuscript. Zhao-jia WANG and Tian-yong HUANG helped to organize the manuscript. Ru WANG and Yu-sheng FAN revised and edited the final version.

### Conflict of interest

Ru WANG, Yu-sheng FAN, Zhao-jia WANG, Tian-yong HUANG, and Tao ZHANG declare that they have no conflict of interest.

### References

Aboelkheir M, Siqueira CYS, Souza Jr FG, et al., 2018. Influence of styrene-butadiene co-polymer on the hydration kinetics of SBR-modified well cement slurries. *Macromolecular Symposia*, 380(1):1800131.

- <https://doi.org/10.1002/masy.201800131>
- Ali MB, Saidur R, Hossain MS, 2011. A review on emission analysis in cement industries. *Renewable and Sustainable Energy Reviews*, 15(5):2252-2261.  
<https://doi.org/10.1016/j.rser.2011.02.014>
- Assaad JJ, 2018. Development and use of polymer-modified cement for adhesive and repair applications. *Construction and Building Materials*, 163:139-148.  
<https://doi.org/10.1016/j.conbuildmat.2017.12.103>
- ASTM (American Society for Testing and Materials), 2002. Standard Practice for Maintaining Constant Relative Humidity by Means of Aqueous Solutions, ASTM E104-02. ASTM International, USA.
- Barbarulo R, Peycelon H, Prené S, et al., 2005. Delayed ettringite formation symptoms on mortars induced by high temperature due to cement heat of hydration or late thermal cycle. *Cement and Concrete Research*, 35(1): 125-131.  
<https://doi.org/10.1016/j.cemconres.2004.05.041>
- Beeldens A, van Gemert D, Schorn H, et al., 2005. From microstructure to macrostructure: an integrated model of structure formation in polymer-modified concrete. *Materials and Structures*, 38(6):601-607.  
<https://doi.org/10.1007/BF02481591>
- Berger S, Coumes CCD, le Bescop P, et al., 2011. Influence of a thermal cycle at early age on the hydration of calcium sulfoaluminate cements with variable gypsum contents. *Cement and Concrete Research*, 41(2):149-160.  
<https://doi.org/10.1016/j.cemconres.2010.10.001>
- Cai GC, Zhao J, 2016. Application of sulfoaluminate cement to repair deteriorated concrete members in chloride ion rich environment—a basic experimental investigation of durability properties. *KSCE Journal of Civil Engineering*, 20(7):2832-2841.  
<https://doi.org/10.1007/s12205-016-0130-4>
- Cao QY, Sun W, Guo LP, et al., 2012. Polymer-modified concrete with improved flexural toughness and mechanism analysis. *Journal of Wuhan University of Technology-Materials Science Edition*, 27(3):597-601.  
<https://doi.org/10.1007/s11595-012-0512-5>
- Cao QY, Hao TY, Sun W, 2013. Study on polymer-modified concrete for improving flexural toughness. *Applied Mechanics and Materials*, 405-408:2815-2819.  
<https://doi.org/10.4028/www.scientific.net/amm.405-408.2815>
- CBMC (China Building Material Council), 2005. Cementitious Self-leveling Floor Mortar, JC/T 985-2005. National Development and Reform Commission, Beijing, China (in Chinese).
- Chung DDL, 2004. Use of polymers for cement-based structural materials. *Journal of Materials Science*, 39(9):2973-2978.  
<https://doi.org/10.1023/B:JMSE.0000025822.72755.70>
- Eren F, Gödek E, Keskinates M, et al., 2017. Effects of latex modification on fresh state consistency, short term strength and long term transport properties of cement mortars. *Construction and Building Materials*, 133:226-233.  
<https://doi.org/10.1016/j.conbuildmat.2016.12.080>
- GAQSIQ (General Administration of Quality Supervision, Inspection and Quarantine of the People's Republic of China), 2005. Test Method for Fluidity of Cement Mortar, GB/T 2419-2005. Standardization Administration of the People's Republic of China, Beijing, China (in Chinese).
- Glasser FP, Zhang L, 2001. High-performance cement matrices based on calcium sulfoaluminate–belite compositions. *Cement and Concrete Research*, 31(12):1881-1886.  
[https://doi.org/10.1016/S0008-8846\(01\)00649-4](https://doi.org/10.1016/S0008-8846(01)00649-4)
- Han DD, Chen WD, Zhong SY, 2018. Physical retardation mechanism of latex polymer on the early hydration of cement. *Advances in Cement Research*, 30(3):113-122.  
<https://doi.org/10.1680/jadcr.17.00055>
- ISO (International Organization for Standardization), 2002. Hygrothermal Performance of Building Materials and Products—Determination of Water Absorption Coefficient by Partial Immersion, ISO 15148-2002. ISO, Geneva, Switzerland.
- ISO (International Organization for Standardization), 2009. Cement—Test Methods—Determination of Strength, ISO 679-2009. ISO, Geneva, Switzerland.
- Juenger MCG, Winnefeld F, Provis JL, et al., 2011. Advances in alternative cementitious binders. *Cement and Concrete Research*, 41(12):1232-1243.  
<https://doi.org/10.1016/j.cemconres.2010.11.012>
- Kim MO, 2020. Influence of polymer types on the mechanical properties of polymer-modified cement mortars. *Applied Sciences*, 10(3):1061.  
<https://doi.org/10.3390/app10031061>
- Li L, Wang R, 2021. Early hydration of CSA cement modified with styrene–butadiene copolymer dispersion. *Advances in Cement Research*, 33(1):14-27.  
<https://doi.org/10.1680/jadcr.19.00038>
- Li L, Wang R, Lu QY, 2018. Influence of polymer latex on the setting time, mechanical properties and durability of calcium sulfoaluminate cement mortar. *Construction and Building Materials*, 169:911-922.  
<https://doi.org/10.1016/j.conbuildmat.2018.03.005>
- Li L, Wang R, Zhang SK, 2019. Effect of curing temperature and relative humidity on the hydrates and porosity of calcium sulfoaluminate cement. *Construction and Building Materials*, 213:627-636.  
<https://doi.org/10.1016/j.conbuildmat.2019.04.044>
- Li L, Peng Y, Wang R, et al., 2020. The effect of polymer dispersions on the early hydration of calcium sulfoaluminate cement. *Journal of Thermal Analysis and Calorimetry*, 139(1):319-331.  
<https://doi.org/10.1007/s10973-019-08413-3>
- Liao YS, Wei XS, Li GW, 2011. Early hydration of calcium sulfoaluminate cement through electrical resistivity measurement and microstructure investigations. *Construction*

- and *Building Materials*, 25(4):1572-1579.  
<https://doi.org/10.1016/j.conbuildmat.2010.09.042>
- Liu J, Xu CW, Zhu XY, et al., 2003. Modification of high performances of polymer cement concrete. *Journal of Wuhan University of Technology-Materials Science Edition*, 18(1):61-64.  
<https://doi.org/10.1007/BF02835091>
- Lu LC, Lu ZY, Liu SQ, et al., 2009. Durability of alite-calcium barium sulphoaluminate cement. *Journal of Wuhan University of Technology-Materials Science Edition*, 24(6):982-985.  
<https://doi.org/10.1007/s11595-009-6982-4>
- Mehta PK, 1972. Stability of ettringite on heating. *Journal of the American Ceramic Society*, 55(1):55-57.  
<https://doi.org/10.1111/j.1151-2916.1972.tb13403.x>
- Moradi SST, Nikiolaev NI, Leusheva EL, 2018. Improvement of cement properties using a single multi-functional polymer. *International Journal of Engineering*, 31(1):181-187.  
<https://doi.org/10.5829/ije.2018.31.01a.24>
- Nishikawa T, Suzuki K, Ito S, 1992. Decomposition of synthesized ettringite by carbonation. *Cement and Concrete Research*, 22(1):6-14.  
[https://doi.org/10.1016/0008-8846\(92\)90130-N](https://doi.org/10.1016/0008-8846(92)90130-N)
- Peng JH, Zhang JX, Qu JD, 2006. The mechanism of the formation and transformation of ettringite. *Journal of Wuhan University of Technology-Materials Science Edition*, 21(3):158-161.  
<https://doi.org/10.1007/BF02840908>
- Poon CS, Groves GW, 1987. The effect of latex on macrodefect-free cement. *Journal of Materials Science*, 22(6):2148-2152.  
<https://doi.org/10.1007/BF01132951>
- Qian XQ, Zhan SL, 2002. Enhancement of durability of glass fiber-reinforced cement with PVA. *Journal of Zhejiang University-SCIENCE A*, 3(2):181-187.  
<https://doi.org/10.1631/jzus.2002.0181>
- Qiu GH, Xu Y, Shi ZL, et al., 2010. Feasibility analysis on utilization of coal gangue as clay for cement. *Journal of Zhejiang University (Engineering Science)*, 44(5):1003-1008 (in Chinese).  
<https://doi.org/10.3785/j.issn.1008-973X.2010.05.028>
- Ramli M, Tabassi AA, Hoe KW, 2013. Porosity, pore structure and water absorption of polymer-modified mortars: an experimental study under different curing conditions. *Composites Part B: Engineering*, 55:221-233.  
<https://doi.org/10.1016/j.compositesb.2013.06.022>
- Sharp JH, Lawrence CD, Yang R, 1999. Calcium sulfoaluminate cements—low-energy cements, special cements or what? *Advances in Cement Research*, 11(1):3-13.  
<https://doi.org/10.1680/adcr.1999.11.1.3>
- Shi C, Zou XW, Yang L, et al., 2020. Influence of humidity on the mechanical properties of polymer-modified cement-based repair materials. *Construction and Building Materials*, 261:119928.  
<https://doi.org/10.1016/j.conbuildmat.2020.119928>
- Shi HS, Deng K, Yuan F, et al., 2009. Preparation of the saving-energy sulphoaluminate cement using MSWI fly ash. *Journal of Hazardous Materials*, 169(1-3):551-555.  
<https://doi.org/10.1016/j.jhazmat.2009.03.134>
- Singh M, Kapur PC, Pradip, 2008. Preparation of calcium sulphoaluminate cement using fertiliser plant wastes. *Journal of Hazardous Materials*, 157(1):106-113.  
<https://doi.org/10.1016/j.jhazmat.2007.12.117>
- Tan B, Okoronkwo MU, Kumar A, et al., 2020. Durability of calcium sulfoaluminate cement concrete. *Journal of Zhejiang University-SCIENCE A (Applied Physics & Engineering)*, 21(2):118-128.  
<https://doi.org/10.1631/jzus.A1900588>
- Wang M, Wang RM, Zheng SR, et al., 2015. Research on the chemical mechanism in the polyacrylate latex modified cement system. *Cement and Concrete Research*, 76:62-69.  
<https://doi.org/10.1016/j.cemconres.2015.05.008>
- Wang MJ, Li HD, Zeng Q, et al., 2020. Effects of nanoclay addition on the permeability and mechanical properties of ultra high toughness cementitious composites. *Journal of Zhejiang University-SCIENCE A (Applied Physics & Engineering)*, 21(12):992-1007.  
<https://doi.org/10.1631/jzus.A2000023>
- Wang PM, Li N, Xu LL, 2017. Hydration evolution and compressive strength of calcium sulphoaluminate cement constantly cured over the temperature range of 0 to 80 °C. *Cement and Concrete Research*, 100:203-213.  
<https://doi.org/10.1016/j.cemconres.2017.05.025>
- Wang R, Li J, Zhang T, et al., 2016. Chemical interaction between polymer and cement in polymer-cement concrete. *Bulletin of the Polish Academy of Sciences Technical Sciences*, 64(4):785-792.  
<https://doi.org/10.1515/bpasts-2016-0087>
- Wang R, Li L, Xu YD, 2019. Influence of curing regimes on the mechanical properties, water capillary adsorption, and microstructure of CSA cement mortar modified with styrene-butadiene copolymer dispersion. *Journal of Materials in Civil Engineering*, 31(1):04018344.  
[https://doi.org/10.1061/\(ASCE\)MT.1943-5533.0002553](https://doi.org/10.1061/(ASCE)MT.1943-5533.0002553)
- Wang XB, Pan ZH, Shen XD, et al., 2016. Stability and decomposition mechanism of ettringite in presence of ammonium sulfate solution. *Construction and Building Materials*, 124:786-793.  
<https://doi.org/10.1016/j.conbuildmat.2016.07.135>
- Winnefeld F, Lothenbach B, 2010. Hydration of calcium sulfoaluminate cements—experimental findings and thermodynamic modelling. *Cement and Concrete Research*, 40(8):1239-1247.  
<https://doi.org/10.1016/j.cemconres.2009.08.014>
- Xu F, Zhou MK, Li BX, et al., 2010. Influences of polypropylene fiber and SBR polymer latex on abrasion resistance of cement mortar. *Journal of Wuhan University of Technology-Materials Science Edition*, 25(4):624-627.

- <https://doi.org/10.1007/s11595-010-0057-4>  
Yang ZX, Shi XM, Creighton AT, et al., 2009. Effect of styrene-butadiene rubber latex on the chloride permeability and microstructure of Portland cement mortar. *Construction and Building Materials*, 23(6):2283-2290.  
<https://doi.org/10.1016/j.conbuildmat.2008.11.011>
- Zhang DC, Xu DY, Cheng X, et al., 2009. Carbonation resistance of sulphoaluminate cement-based high performance concrete. *Journal of Wuhan University of Technology-Materials Science Edition*, 24(4):663-666.
- <https://doi.org/10.1007/s11595-009-4663-y>  
Zhang L, Glasser FP, 2002. Hydration of calcium sulfoaluminate cement at less than 24 h. *Advances in Cement Research*, 14(4):141-155.  
<https://doi.org/10.1680/adcr.2002.14.4.141>
- Zhong SY, Chen ZY, 2002. Properties of latex blends and its modified cement mortars. *Cement and Concrete Research*, 32(10):1515-1524.  
[https://doi.org/10.1016/S0008-8846\(02\)00813-X](https://doi.org/10.1016/S0008-8846(02)00813-X)